HIGHLY SENSITIVE DETECTION OF Cr(VI), Pb(II) AND Cd(II) IONS BY A NEW FLUORESCENT SENSOR BASED ON 4-AMINO-3-HYDROXYNAPHTHALENE SULFONIC ACID-DOPED POLYPYRROLE

Mohamed Lamine Sall[1,2], Abdou Karim Diagne Diaw[1], Diariatou Gningue-Sall[1], Mehmet Ali Oturan[2], Jean-Jacques Aaron[2]*

[1]*Laboratoire de Chimie Physique Organique et d'Analyse Instrumentale, Département de Chimie, Université Cheikh Anta Diop, Dakar BP 5005, Dakar-Fann, Sénégal*
[2]*Université Paris-Est marne-la-Vallée, Laboratoire Géomatériaux et Environnement (LGE), EA4508, 77454 Marne-la-Vallée, France*
jeanjacquesaaron@yahoo.fr

A new electrosynthesized, fluorescent 4-amino-3-hydroxynaphthalene-1-sulfonic acid-doped polypyrrole (AHNSA-PPy) was used for the detection of Cr(VI), Pb(II) and Cd(II) heavy metallic ions. The optical properties of AHNSA-PPy were studied by UV-VIS absorption and fluorescence spectrometry in diluted DMSO solutions. UV-VIS spectrum showed a main band at 260 nm, a moderate band at 240 nm, and shoulders at 285, 295, 320 and 360 nm, whereas the fluorescence spectrum presented an excitation peak at 330 nm and a main emission peak at 390 nm with a shoulder at 295 nm. The effects of heavy metallic ions, including Cr(VI), Pb(II), and Cd(II), on the AHNSA-PPy UV-VIS absorption and fluorescence spectra were investigated. AHNSA-PPy fluorescence spectra were strongly quenched upon increasing the Cr(VI), Pb(II) and Cd(II) concentrations. Linear Stern-Volmer relationships were established, and polynomial equations for Pb(II) and Cd(II) were obeyed, indicating the existence of a AHNSA-PPy dynamic fluorescence quenching mechanism for Cr(VI) and a combination of dynamic and static fluorescence quenching for Pb(II) and Cd(II). The AHNSA-PPy sensor showed high sensitivity for fluorescence detection of the three heavy metallic ions, with very low limits of detection (3σ) of 1.4 nM for Cr(VI), 2.7 nM for Cd(II) and 2.6 nM for Pb(II). Therefore, this very sensitive quenching fluorimetric sensor is proposed for the detection of trace, toxic heavy metallic ions in the environment.

Keywords: 4-amino-3-hydroxynaphthalene-1-sulfonic acid-doped polypyrrole (AHNSA-P Py); Cr(VI), Pb(II) and Cd(II); fluorescence sensor; quenching fluorimetric method

ВИСОКО СЕНЗИТИВНА ДЕТЕКЦИЈА НА ЈОНИ НА Cr(VI), Pb(II), И Cd(II) СО НОВ ФЛУОРЕСЦЕНТЕН СЕНЗОР ЗАСНОВАН НА 4-АМИНО-3-ХИДРОКСИНАФТЕЛЕН СУЛФОНСКА КИСЕЛИНА СО ПРИМЕСА НА ПОЛИПИРОЛ

Беше применета нова електросинтетизирана флуоресцентна 4-амино-3-хидроксинафтален-1-сулфонска киселина со примеси на полипирол (AHNSA-PPy) за детекција на тешките метални јони на Cr(VI), Pb(II) и Cd(II). Оптичките својства на AHNSA-PPy беа испитани со UV-VIS апсорпциона и флуоресцентна спектрометрија во раствори разредени со DMSO. UV-VIS спектарот покажува главна лента на 260 nm, умерена лента на 240 nm и преслап на 285, 295, 320 и 360 nm, додека флуоресцентниот спектар покажува ексцитациски пик на 330 nm и главен емисионен пик на 390 nm со преслап на 295 nm. Со UV-VIS апсорпциони и флуоресцентни спектри беа испитани ефектите на металните јони, вклучувајќи ги Cr(VI), Pb(II) и Cd(II), врз AHNSA-PPy. Флуоресцентните спектри на AHNSA-PPy се придушуваат со зголемување на концентрациите на Cr(VI), Pb(II) и Cd(II). Беа утврдени линеарни зависности од типот Stern-Volmer, додека Pb(II) и Cd(II) се покоруваат на полиномни равенки, што укажува на постоење динамично флуоресцентно

придушување на AHNSA-PPy за Cr(VI) и комбинација на динамично и статично флуоресцентно придушување за Pb(II) и Cd(II). Сензорот AHNSA-PPy покажува висока сензитивност за флуоресцентна детекција на овие три вида тешки метални јони, со многу низок праг на детекција (3σ) од 1,4 nM за Cr(VI), 2,7 nM за Cd(II) и 2,6 nM за Pb(II). Од овие причини овој многу осетлив сензор се предлага за детекција на трагови на токсични тешки метални јони во животната средина.

Клучни зборови: 4-амино-3-хидроксинафтален-1-сулфонска киселина со примеса на полипирол (AHNSA-P Py); Cr(VI), Pb(II) и Cd(II); флуоресцентен сензор; флуориметриски метод на придушување

1. INTRODUCTION

The development of chemical sensors for heavy metal ions has attracted increasing interest because of the toxic effects of these pollutants on human health and the environment [1, 2]. Even at very low concentrations, these heavy metals are extremely toxic and often resist conventional treatments. They, therefore, degrade the quality of drinking water resources and cause serious illnesses. In fact, numerous studies have shown the presence of these contaminants in marine waters and ecosystems and their impact on aquatic environments [3–7]. Generally, chromium, cadmium and lead are considered the most dangerous heavy metals.

For example, chromium can cause brain development disorders in children, leading to psychological disturbances and learning difficulties. It can easily enter human cells; can provoke severe damage to the liver, kidneys and other organs; and is highly carcinogenic [8–10]. Chronic intoxication by chromium produces skin lesions and mucous, as well as breathing difficulties and even bronchopulmonary cancers. The most common chromium oxidation states are trivalent Cr(III) and hexavalent Cr(VI), with Cr(VI) being 1000 times more toxic than Cr(III) [11, 12].

Lead can decrease human fertility and lead to neurological, cardiovascular and gastrointestinal disorders. Also, it can increase the mortality of fetuses, often from spontaneous abortion. In children, lead can cause nervous system disorders, anemia, behavioral problems, kidney problems, hearing loss and lower intelligence quotients. In addition, this metal has mutagenic and carcinogenic properties [13–15] and is highly ecotoxic [16].

Cadmium can yield kidney problems and increase blood pressure [17]. Moreover, its inhalation is very dangerous and can even be lethal because it enters human cells and accumulates in high concentrations in the cytoplasmic and nuclear spaces [18, 19]. Also, it is very toxic, even at low doses, for many animal and plant species, aquatic and terrestrial [20]. Therefore, highly sensitive fluorescent sensors have been developed for the efficient detection and recognition of toxic heavy metallic ions, such as Hg(II), Zn(II), Al(III), and Cr(VI), in order to determine the level of metallic pollution of natural waters [21–23].

Conjugated polymers (CPs) are interesting materials with important photophysical properties related to their structure, which can lead to a number of applications in optoelectronics and biosensors [24–26]. For example, Kim [24] has shown intermolecular and intramolecular effects on the photophysical properties of CPs. Scheblykin *et al.* [25] have studied the photophysics and excited state dynamics of CPs, and Cabarcos *et al.* [26] have characterized photoluminescence quenching of mixed water-soluble CPs by oxygen and polymers, evaluating their potential usefulness as biosensor materials. Also, the fluorescence quenching of two coumarin-3-carboxylic acids by trivalent lanthanide ions has been investigated by Cisse *et al.* [27].

Conductive organic polymers (COPs) have been rarely applied as fluorescent sensors to determine low concentrations of heavy metals in solution [26, 28–30] In most cases, the determination of heavy metals was based on increased fluorescence quenching of COPs with heavy metal ion concentration, produced by interactions between the two components. Depending on the type of COP-heavy metal interaction, two main fluorescence quenching mechanisms were found: dynamic, resulting from collisions between a fluorescent COP and heavy metal ions, or static, due to the formation of a non-fluorescent complex between the polymer and metallic ions.

In order to evaluate traces of heavy metals in solution, several authors have utilized quenching of COP fluorescence intensity (I_F) when heavy metal concentration was progressively increased. For instance, Maiti *et al.* [31] investigated the evolution of poly(thiophene-3-yl-acetic acid 8-quinolinyl ester) fluorescence intensity upon adding low concentrations of metal ions, such as aluminum, cadmium, zinc, copper and lead, and ob-

served dynamic fluorescence quenching. They obtained linear Stern-Volmer relationships, with Stern-Volmer constants of 2.3×10^3–7×10^4 M^{-1} [31]. In another study, Holt *et al.* [32] chemically synthesized and grafted thin films of polythiophene (PT) and poly-3-hexylthiophene (P3HT) onto optically transparent substrates. These films formed complexes with traces of ferric chloride and iodine, resulting into static fluorescence quenching, indicated by downward curved Stern-Volmer plots [32]. Also, Xing *et al.* [33] synthesized a new series of water-soluble cationic polyfluorene copolymers containing 2,2′-bipyridyl-phenylene-vinylene moieties (PFP-P2), which were used as a sensitive fluorescent probe to detect Cu(II) ions in aqueous medium. Upon adding Cu(II) ions, the strong fluorescence of PFP-P2 was efficiently quenched, leading to a non-linear Stern-Volmer relationship [33]. Very recently, our group developed a new fluorescent sensor based on the fluo-rescence quenching of benzene sulfonic acid-doped polypyrrole films for extremely sensitive detection of Cu(II) and Pb(II) ions [34].

Considering these literature results, we investigated the UV-VIS absorption and fluorescence spectral properties, in DMSO, of a novel 4-amino-3-hydroxynaphthalene-1-sulfonic acid-doped polypyrrole (AHNSA-PPy) film, previously electrosynthesized and characterized by us (Scheme 1) [35]. Then, we proposed several quantitative treatments of AHNSA-PPy fluorescence quenching by three heavy metallic ions, Cr(VI), Pb(II) and Cd(II), chosen among the most toxic and most used heavy metals, in order to demonstrate the usefulness of our approach. Finally, we developed a simple, reliable, rapid, and sensitive fluorescent sensor based on AHNSA-PPy for the determination of Cr(VI), Pb(II) and Cd(II) ion concentrations by a quenching spectrofluorimetric method.
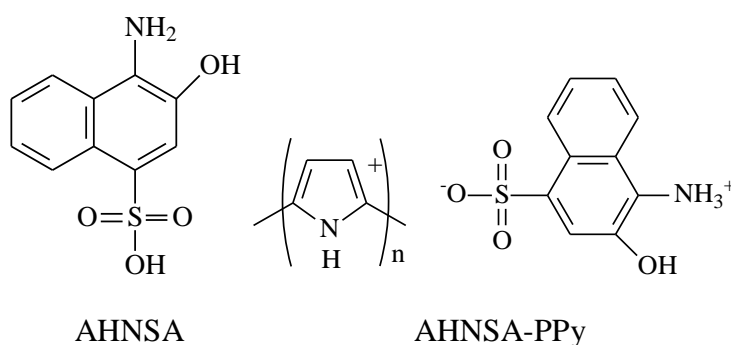
Scheme 1. Molecular structures of AHNSA and AHNSA-PPy

2. EXPERIMENTAL

2.1. *Chemicals*

Pyrrole (Py, 99 %), 4-amino-3-hydroxynaphthalene-1-sulfonic acid (AHNSA), sodium hydroxide (NaOH), dimethylsulfoxide (DMSO), dimethyl formamide (DMF), potassium dichromate ($K_2Cr_2O_7$), cadmium sulfate ($CdSO_4$) and lead nitrate [$Pb(NO_3)_2$] were obtained from Sigma-Aldrich and used as received.

2.2. *Electrochemical measurements*

For the electrosynthesis of AHNSA-PPy films [35], electrochemical measurements were carried out in a single compartment, three-electrode cell at room temperature, using an EG & G Princeton Applied Research PAR 362 model potentiostat/galvanostat, equipped with a Kipp & Zonen X-Y recorder. A steel plate was used as the working electrode, while a stainless-steel grid and saturated calomel electrode (SCE) were employed, respectively, as counter and reference electrodes. XPS analysis of the polymer led to an AHNSA doping percentage of 28.8% in the electrosynthesized AHNSA-PPy films.

2.3. *Spectral measurements*

UV-VIS absorption spectra of AHNSA-PPy were determined on a Perkin-Elmer Lambda 2 UV-VIS absorption spectrophotometer at room temperature in DMSO and DMF solutions. The uncorrected excitation and emission fluorescence spectra were recorded with a Kontron SFM-25 spectrofluorimeter, interfaced with a microcomputer, at room temperature in DMSO solution, using slit widths of 10 nm.

2.4. *Analytical procedure for the determination of heavy metal ions*

An AHNSA-PPy/DMSO solution (3.4×10^{-5} r.u. (repeat unit) l^{-1}) was prepared and utilized for the determination of Cr(VI), Pb(II) and Cd(II) ions. Microvolumes (20 µl) of aqueous solutions containing increasing Cr(VI), Pb(II) or Cd(II) concentrations between 0 and 100 µM were added to a constant volume (2 ml) of the AHNSA-PPy/DMSO solution. Then, the evolution of the UV-VIS absorption spectra or of the fluorescence emission spectra of AHNSA-PPy was monitored at different Cr(VI), Pb(II) or Cd(II) concentrations.

The AHNSA-PPy (10^{-5} r.u. l^{-1}) fluorescence emission spectra ($\lambda_{ex} = 330$ nm) in DMSO, obtained at different Cr(VI), Pb(II) or Cd(II) concentrations, were recorded, and the maximum emission fluorescence intensity values were plotted against the Cr(VI), Pb(II) or Cd(II) concentrations from 0 to 31.2 µM. Several quantitative treatments were used to determine the type of AHNSA-PPy fluorescence quenching.

For example, in the case of lead, we solubilized 0.4 mg of $Pb(NO_3)_2$ in 5 ml of DMSO, corresponding to solution concentration of 2.10^{-4} M Pb(II). Then, we collected, respectively, 6, 10, 200 and 500 µl of this solution, which were introduced into 3 ml of AHNSA-PPy solution, giving Pb(II) concentrations of 0.4, 0.67, 12.5 and 31.2 µM, respectively.

2.5. *Quantitative treatments of AHNSA-PPy fluorescence quenching*

In order to elucidate the nature of the fluorescence quenching mechanism(s) (*i.e.* dynamic and/or static interactions), several equations were proposed for studying the concentration effects of Cr(VI), Pb(II), or Cd(II) ions on the AHNSA-PPy fluorescence intensity. Therefore, an increase in the I_0/I ratio (fluorescence intensity in the absence of quencher/fluorescence intensity in the presence of quencher) with quencher concentration gives information on the association between the polymer and quencher in solution. This association can generally occur either by 1) collisions between the quencher molecules and the fluorescent polymer (dynamic fluorescence quenching), 2) by formation of a ground-state, non-fluorescent complex between the polymer and quencher (static fluorescence quenching), or 3) by a combination of both fluorescence quenching mechanisms.

In the case of a completely dynamic quenching mechanism, a linear, classical Stern-Volmer relation was observed [26]:

$$I_0/I = 1 + K_{SV}[Q], \qquad (1)$$

where I_0 is the AHNSA-PPy fluorescence intensity in the absence of quencher, I is the AHNSA-PPy fluorescence intensity in the presence of quencher, K_{SV} is the Stern-Volmer constant (in $1\ M^{-1}$), and [Q] is the quencher [Cr(VI), Pb(II) or Cd(II)] concentration.

In the case of a purely static quenching mechanism [26, 27], the experimental results generally obeyed the Perrin equation:

$$\log\left(\frac{I_0}{I}\right) = V_q N_A [Q] = K_S [Q] \qquad (2)$$

where V_q is the volume surrounding the fluorophore, N_A is Avogadro's number, and K_S is the static quenching constant ($K_S = V_q N_A$).

When the dynamic and static quenching mechanisms occurred simultaneously, the Stern-Volmer and Perrin plots were not linear. A polynomial equation was observed when static quenching was characterized by the formation of a non-fluorescent 1:1 complex [27]:

$$I_0/I = (1 + K_{SV}[Q])(1 + K_S[Q]) = 1 + (K_{SV} + K_S)[Q] + K_{SV} K_S [Q]^2, \qquad (3)$$

where K_{SV} and K_S are the dynamic quenching and static quenching constants, respectively. When I_0/I was plotted against [Q], an upward curvature was observed. It was possible to calculate the $K_{SV} + K_S$ values using the fit of the curve and equation (3).

The limit of detection (LOD) was calculated by plotting the calibration curve $\Delta I = I_0 - I = f([Q])$ for each heavy metallic ion and applying the following equation:

$$LOD = 3\ \sigma/k,$$

where σ is the standard deviation of blank measurements, and k is the slope of the linear fit in the fluorescence titration.

3. RESULTS AND DISCUSSION

3.1. *UV-VIS absorption spectral study*

We recorded the UV-VIS absorption spectrum of a DMSO solution of 3.4×10^{-5} r.u. l^{-1}

AHNSA-PPy (oxidized polymer film, obtained by CV with five cycles) at room temperature (Fig. 1). This AHNSA-PPy UV-VIS spectrum exhibited a weak band around 240 nm (log ε = 3.92), a very intense band at 260 nm (log ε = 4.43), and weak shoulders at 285 nm (log ε = 4.01), 295 nm (log ε = 4.02), 320 nm (log ε = 4.01) and 360 nm (log ε = 4.03); (Fig. 1).

Upon comparing this AHNSA-PPy UV-VIS spectrum in DMSO with the one previously obtained in DMF [35], we found the absorption spectra in both solvents were similar. Therefore, we were able to attribute the short wavelength absorption bands at 240 and 260 nm, observed in DMSO, to π-π* electronic transitions of the Py ring in the AHNSA-PPy conjugated heteroaromatic system. Moderate blue shifts of, respectively, 15 and 25 nm occurred for these bands in DMSO relative to those in DMF [255 (log ε = 3.94) and 285 nm (log ε = 4.10)], which might be due to differences in polarity of the two solvents. The weak long wavelength shoulders, appearing at 285, 295, 320 and 360 nm, which were blue-shifted relative to DMF, probably corresponded to less intense electronic n-π* transitions of the naphthalene SO_3H and NH_2 substituents, confirming the insertion of AHNSA between the PPy chains [35].
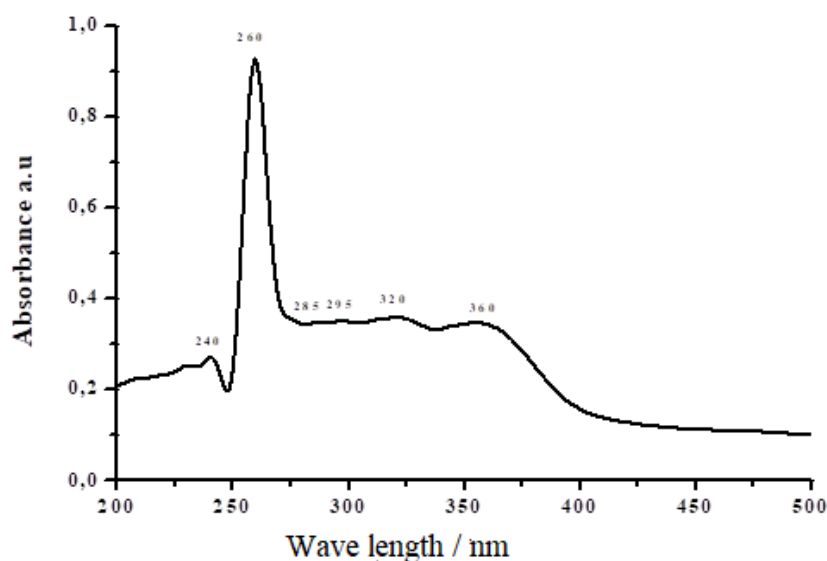
Fig. 1. UV-VIS absorption spectrum of AHNSA-PPy (3.4×10^{-5} r.u. l^{-1}) in DMSO at room temperature

3.2. *Fluorescence spectral study*

The fluorescence excitation and emission spectra of AHNSA and AHNSA-PPy (polymer oxidized film obtained by CV with five cycles) were recorded in dilute DMSO solutions at room temperature (Table 1 and Fig. 2).

The fluorescence excitation spectrum of AHNSA exhibited one main, wide band, with a peak around 345 nm and a shoulder at about 300 nm, whereas the emission spectrum possessed only one peak at 435 nm (Table 1 and Fig. 2). The fluorescence excitation spectrum of AHNSA-PPy also displayed a main band, appearing at 330 nm, and a shoulder around 295 nm, whereas the emission spectrum possessed only one band at 390 nm (Table 1 and Fig. 2). We observed notable blue shifts for the excitation ($\Delta\lambda_{ex}$ = –15 nm) and emission ($\Delta\lambda_{em}$ = –45 nm) spectra when going from AHNSA (monomer) to AHNSA-PPy (polymer). These results indicated the existence of significant intermolecular interactions between AHNSA, under the amphoteric salt form, and the PPy chain and confirmed that the AHNSA naphthalenic group was not involved in the electropolymerization process but was simply inserted between the polypyrrolic chains. For AHNSA, as well as for the AHNSA-PPy polymer, the excitation maxima occurred at wavelength values relatively close to the UV-VIS absorption spectra, suggesting that the fluorescent species were also responsible for the absorption (Table 1).

The AHNSA-PPy polymer fluorescence excitation and emission spectra in DMF [35] and DMSO diluted solutions (Figs. 2A and 2B) presented very similar features in both solvents, with moderate shifts of about 5 to 15 nm. However, the bands were sharper with higher fluorescence intensities, and more pronounced band distortion was observed in DMSO than in DMF, which might be attributed to solvent polarity effects.

T a b l e 1

Fluorescence excitation and emission spectra
of AHNSA and AHNSA-PPy polymer in DMF and DMSO.[a]

Compound	Solvent	λ_{ex} (nm)		λ_{em} (nm)
AHNSA	DMF[b]	300[c]	345	430
AHNSA	DMSO	300[c]	345	435
AHNSA-PPy	DMF[b]	290[c]	335	406
AHNSA-PPy	DMSO	295[c]	330	390

[a] Concentrations: AHNSA-PPy = 10^{-6} r.u. l^{-1}; AHNSA = 10^{-6} M in DMF and DMSO.
[b] From Ref. [35]. [c] Shoulder.
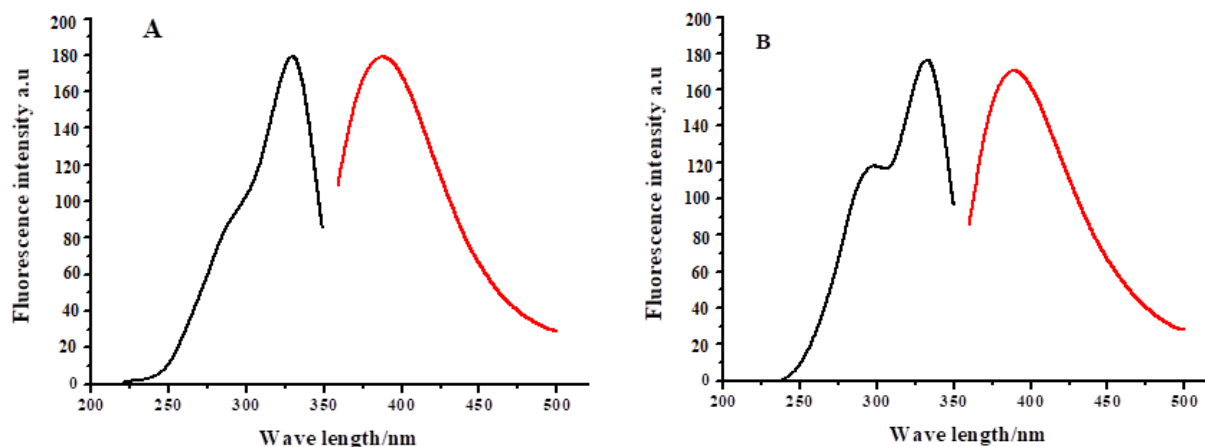
Fig. 2. Fluorescence excitation and emission spectra of an AHNSA-PPy film in:
A) DMF (3.4×10^{-5} r.u.l^{-1}) [35] and B) DMSO (10^{-5} r.u. l^{-1}) at room temperature.

3.3. *Effects of heavy metallic ions on the optical properties of AHNSA-PPy*

3.3.1. *Effects of heavy metallic ions on the AHNSA-PPy UV-VIS absorption spectra*

We followed the evolution of the AHNSA-PPy UV-VIS absorption spectra in DMSO solution at room temperature in the presence of increasing concentrations of heavy metallic ions, including Cr(VI), Pb(II), and Cd(II), from 0 to 100 µM (Figs. 3A–3C). The analysis of these AHNSA-PPy absorption spectra showed an important decrease in the intensity of the Py bands appearing at about 240 and 260 nm, as well as those due to the naphthalene SO₃H, OH, and NH₂ substituents, located at approximately 285, 295, 320, and 360 nm (except in the case of chromium). In all cases, the Py absorption bands, observed at 240 and 260 nm, gradually decreased with increases in the heavy metal ion concentration. All these band changes, due to the presence of heavy metal ions, suggested that these ions were linked with the Py units, leading to the formation of non-absorbing complexes between the AHNSA-PPy polymer and heavy metal ions.

Moreover, the ANHSA moiety absorption bands, located at 320 and 360 nm, also underwent a progressive and relatively small decrease with increases in the Pb(II) and Cd(II) concentrations from 0 to 100 µM. This AHNSA moiety absorbance decrease, observed in the presence of Pb(II) and Cd(II), could also be attributed to the formation of non-absorbing complexes, involving the fixation of these heavy metal ions on the SO₃H, OH, and/or NH₂ naphthalenic substituents. However, in contrast with Pb(II) and Cd(II) ions, Cr(VI) ions yielded an apparent increase of the AHNSA moiety absorption bands at wavelengths larger than about 360 nm, which might be explained by a partial overlap of the chromium main absorption band, located at about 350 nm, and of the bands of AHNSA SO₃H, OH, and/or NH₂ substituents.

We also compared the decrease of the AHNSA-PPy absorption maximum, located at 260 nm, upon increasing the heavy metal ion concentration from 0 to 100 µM. This study revealed an absorbance decrease of about 73 % for chromium, 66 % for lead and 64.5 % for cadmium.

The slightly greater AHNSA-PPy absorbance decrease in the presence of chromium suggested slightly better sensitivity of AHNSA-PPy

towards chromium than towards the other metals. However, since the AHNSA-PPy UV-VIS spectra were not extremely sensitive to the variation of heavy metal ion concentrations, we investigated the effect of these ions on the AHNSA-PPy fluorescence spectra.
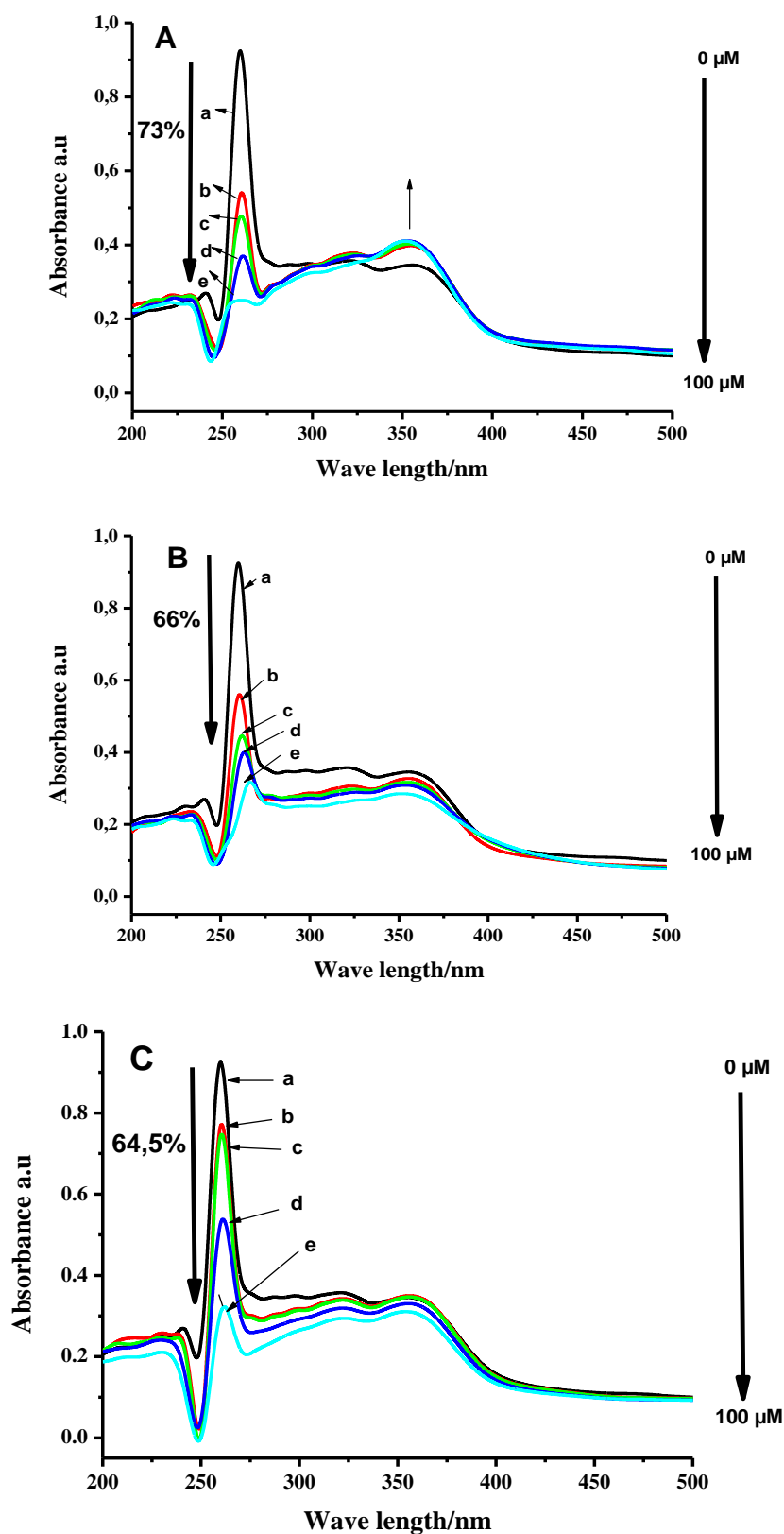
Fig. 3. Effect of (A) Cr(VI), (B) Pb(II) and (C) Cd(II) ion concentrations on the AHNSA-PPy UV-VIS absorption spectra (3.4×10^{-5} r.u. l^{-1}) in DMSO. Heavy metallic ion concentrations: a) 0, b) 10, c) 20, d) 60 and e) 100 μM.

3.3.2. *Effect of heavy metal ions on the AHNSA-PPy fluorescence spectra*

We studied the effects of increasing concentrations of heavy metal ions, including Cr(VI), Pb(II), and Cd(II), from 0 to 31.2 μM on the AHNSA-PPy fluorescence excitation and emission spectra in diluted DMSO solutions at room temperature (Figs. 4A–4C). In all cases, we did not observe any significant change in the shape of wavelength of the polymer excitation and emission fluorescence spectra with increasing heavy metal ion concentration. However, we noted a sharp decrease in the intensity of the fluorescence excitation peaks at about 295 and 330 nm and emission maximum around 390 nm when the heavy metallic ion concentration (Cr(VI), Pb(II) or Cd(II)) increased from 0 to 31.2 μM (Figs. 4A–C).
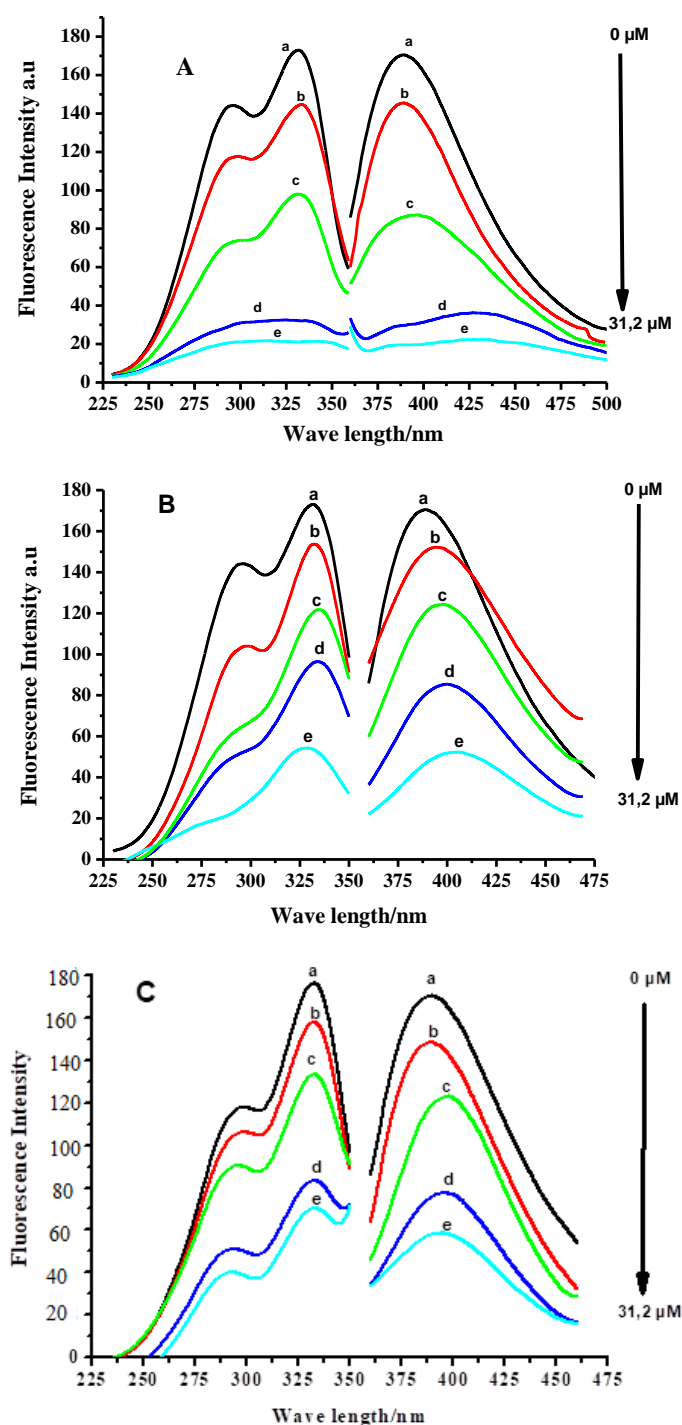
Fig. 4. Effect of **A**) Cr(VI), **B**) Pb(II, and **C**) Cd(II) ion concentrations on AHNSA-PPy fluorescence excitation and emission spectra in DMSO. Heavy metallic ion concentrations: a) 0, b) 0.4, c) 0.64, d) 12.5 and e) 31.2 μM.

This fluorescence quenching of AHNSA-PPy was attributed to interactions of the metal ions with the polymer and was much more pronounced for Cr(VI) than for Pb(II) and Cd(II). This greater fluorescence quenching in the case of hexavalent chromium was consistent with the fact that the amount of Cr(VI) adsorbed per gram of AHNSA-PPy was much greater (maximum adsorption capacity = 224 mg of Cr(VI)/g of polymer) [35] than the amounts of Pb(II) and Cd(II) adsorbed per gram of the same polymer (maximum adsorption capacity = 64 mg of Pb(II) and 50 mg of Cd(II)/g of polymer) [36].

We investigated the fluorescence quenching behavior of AHNSA-PPy with increasing concentrations of Cr(VI), Pb(II) and Cd(II) ions in DMSO. In order to elucidate the nature of this fluorescence quenching, we applied different mathematical treatments, including the Stern-Volmer equation (1), Perrin equation (2), and polynomial equation (3), to our fluorescence quenching results of AHNSA-PPy for the three heavy metal ions under study (Table 2).

Linear Stern-Volmer relationships were established for all heavy metallic ions under study with a good precision, but polynomial equations were also obeyed. Indeed, the correlation coefficient (r) values were satisfactory for both equations. In contrast, the Perrin equation was generally less correctly established, with smaller r values.

The detailed analysis of Stern-Volmer graphs, $I_0/I = f([Q])$, showed the existence of two distinct types of curves, according to the nature of the heavy metallic ion (Figs. 5 A–C and Table 2). For Cr(VI), a strictly linear Stern-Volmer curve was obtained with a r value of 0.995 (Fig. 5A), indicating the dynamic fluorescence quenching of AHNSA-PPy by this metallic ion. In contrast, in the case of Pb(II) and Cd(II), partially linear Stern-Volmer curves were established (r = 0.989 and 0.985, respectively), with two linear domains (Figs. 5B and 5C), suggesting the existence of a more complicated fluorescence quenching mechanism, implying a combination of AHNSA-PPy dynamic and static fluorescence quenching. The difference of linear behavior of the Stern-Volmer curves observed for Cr(VI), on one hand, and for Cd(II) and Pb(II), on the other hand, might also be attributed to the fact that, unlike to Cd^{2+} and Pb^{2+}, hexavalent chromium is an anionic form. Indeed, in the case of Cr(VI), we used the dichromate ion, which should be attached to the positive site of the AHNSA-PPy zwitterionic form, whereas Cd(II) and Pb(II) ions should be fixed to the AHNSA-PPy zwitterionic form negative site.
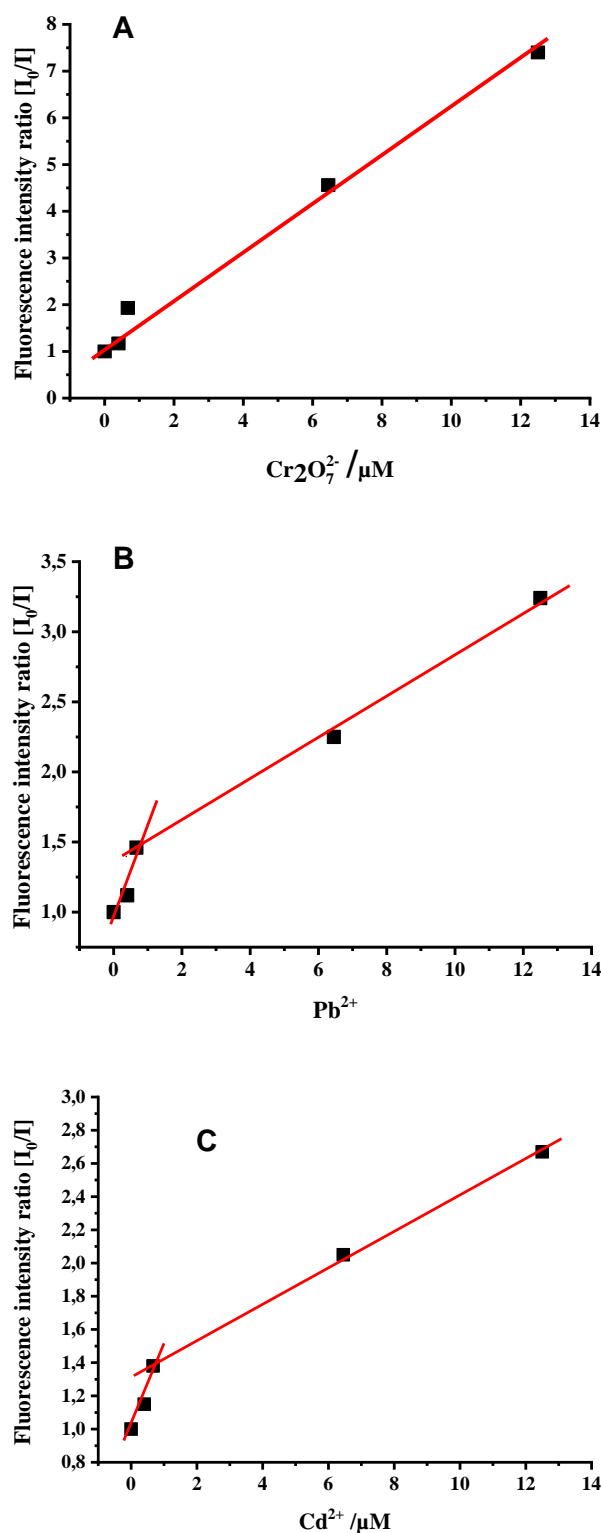
Fig. 5. Stern-Volmer plots of AHNSA-PPy fluorescence intensity ratios [I_0/I] (λ_{em}= 390 nm) in DMSO *vs.* metal ion concentration in μM: **A**) $Cr_2O_7^{2-}$, **B**) Pb^{2+} and **C**) Cd^{2+}.

Similar Stern-Volmer relationships have been reported in other works concerning the fluorescence quenching of substituted coumarins by trivalent lanthanide ions and merocyanine 540 by

biomedically-important salts [27, 37]. Moreover, the polynomial equations displayed *r* values very close to unity, ranging from 0.992 to 0.999, according to the heavy metallic ion, while the Perrin equations exhibited smaller *r* values, between 0.952 and 0.962, indicating that these equations were less well fitted.

The Stern-Volmer constant (K_{SV}) values of AHNSA-PPy were rather high, 1.26×10^5, 1.70×10^5 and 5.02×10^5 M^{-1}, respectively, for Cd(II), Pb(II), and Cr(VI). They were much greater than the corresponding static quenching constant (K_S) values of the Perrin equation, which were 0.32×10^5, 0.38×10^5 and 0.66×10^5 M^{-1} for Cd(II), Pb(II) and Cr(VI), respectively (Table 2). The (K_{SV}

+ K_S) values of the polynomial equations were 0.90×10^5, 1.94×10^5 and 5.78×10^5 M^{-1}, respectively, for Cd(II), Pb(II) and Cr(VI) (Table 2). The larger K_{SV} values compared to the K_S ones indicated the AHNSA-PPy fluorescence dynamic quenching mechanism was more important than the static one, in the case of the three quenchers under study. The observed contribution of a static quenching fluorescence mechanism might be explained by the ground-state formation of non-fluorescent complexes between the Pb(II), Cd(II), or Cr(VI) ions and AHNSA-PPy polymer on one or several active site(s) of the naphthalenic SO$_3$H, OH and NH$_2$ substituents.

T a b l e   2

Quantitative treatments of AHNSA-PPy fluorescence quenching effects by Cr(VI), Pb(II) and Cd(II) metal ions

Ions	Type of quenching	Regression equation [a, b, c]	N[d]	r[e]
Cr(VI)	Dynamic	$I_0/I = 1.20\ (\pm 0.17) + 5.02\ (\pm 0.27)\ 10^5\ [Q]$	5	0.995
	Static	$\log (I_0/I) = 0.11\ (\pm 0.06) + 0.66\ (\pm 0.11)\ 10^5\ [Q]$	5	0.952
	Dynamic + static	$I_0/I = 1.15\ (\pm 0.21) + 5.78\ (\pm 0.29)\ 10^5\ [Q] - 6.35\ (\pm 1.04)\ 10^9\ [Q]^2$	5	0.992
Pb(II)	Dynamic	$I_0/I = 1.13\ (\pm 0.09) + 1.70\ (\pm 0.14)\ 10^5\ [Q]$	5	0.989
	Static	$\log(I_0/I) = 0.06\ (\pm 0.01) + 0.38\ (\pm 0.06)\ 10^5\ [Q]$	5	0.962
	Dynamic + static	$I_0/I = 1.00\ (\pm 0.11) + 1.94\ (\pm 0.69)\ 10^5\ [Q] + 1.97\ (\pm 0.56)\ 10^9\ [Q]^2$	4	0.999
Cd(II)	Dynamic	$I_0/I = 1.14\ (\pm 0.08) + 1.26\ (\pm 0.12)\ 10^5\ [Q]$	5	0.985
	Static	$\log (I_0/I) = 0.06\ (\pm 0.01) + 0.32\ (\pm 0.05)\ 10^5\ [Q]$	5	0.956
	Dynamic + static	$I_0/I = 1\ (\pm 0.09) + 9.03\ (\pm 0.02)\ 10^4\ [Q] + 7.12\ (\pm 0.42)\ 10^{11}\ [Q]^2$	4	0.999

[a] Stern-Volmer equation: $I_0/I = 1 + K_{SV}[Q]$. [b] Perrin equation: $\log(I_0/I) = K_S[Q]$.
[c] Polynomial equation: $I_0/I = 1 + (K_{SV}+K_S)[Q] + K_{SV}K_S[Q]^2$. [d] N = number of data. [e] r = correlation coefficient.

3.3.3. *Evaluation of AHNSA-PPy as a quenching fluorimetric sensor for Cr(VI), Pb(II) and Cd(II) ions*

Using the above-obtained Stern-Volmer relationships, we developed and evaluated a quenching fluorimetric sensor based on AHNSA-PPy fluorescence quenching for the determination of Cr(VI), Pb(II), and Cd(II) ions. We constructed calibration curves of $\Delta I = (I_0 - I)$ *vs.* heavy metallic ion concentration, which showed an increase of ΔI with the metal ion concentration. These calibration curves were linear in the heavy metal ion concentration range under study, with the linear portion of the curves observed from 4×10^{-7} to 12.5×10^{-7} M.

In the case of chromium, the equation of the calibration curve was $\Delta I = -7.84 + 128.7 \times [Cr(VI)]$ with $r = 0.995$. Utilizing a signal-to-noise ratio of three (3σ-IUPAC definition), we calculated a very

low LOD of 1.4 nM for Cr(VI). As seen in Table 3, this LOD value was much lower than those of 0.36 µM found by Zhang *et al.* [23] with a 1,8-naphthalimide-based turn-on fluorescent sensor and 74.9 nM, obtained by Afshani *et al.* [38], using a fluorescent sensor based on a newly synthesized iminocrown ether.

For lead, the calibration curve equation was $\Delta I = -2.77 + 70.2\ [Pb(II)]$ with $r = 0.987$. We also calculated a very low LOD of 2.6 nM. This LOD value was much smaller than the 4 µg/l (19.3 nM) found by Metivier *et al.* [39] with a fluorescent sensor using calixarene-based fluoroionophores bearing two or four dansyl fluorophores. Also, our LOD value was about 240 times smaller than the value of 630 nM obtained by Das *et al.* [40] using a highly selective fluorescent Pb(II) probe based on salicylaldehyde phenylhydrazone (Table 3).

In the case of cadmium, the calibration curve equation was $\Delta I = -1.92 + 72.5$ [Cd(II)] with $r = 0.982$. We obtained a LOD of 2.6 nM. This value was lower than that of 5 nM calculated by Charles *et al.* [41], utilizing an approach based on the fluorescence enhancement of an anthryl-azamacrocycle derivative when chelated to cadmium. Our LOD value was also much smaller than that of 886 μM obtained by Kaya *et al.* [42] using

a highly selective fluorescent sensor for Cd(II) based on poly(azomethine-urethane) (Table 3).

Finally, all our LOD values for Cr(VI) and Cd(II) ions were well below the maximum contaminant levels of 0.1 mg/l for chromium and 0.005 mg/l for cadmium, set by the United States Environmental Protection Agency (US-EPA) for drinking waters [43, 44].

T a b l e 3

Recent literature in fluorescence sensing of metals

Sensor	Metal	LOD	Reference
1,8-Naphthalimide-based turn-on fluorescent sensor	Cr(VI)	0.36 μM	23
3,4:9,10:13,14-Tribenzo-1,12-diaza-5,8-dioxacyclotetradecane-1,11-diene (TBC)	Cr(VI)	74.9 nM	38
Calixarene-based fluoroionophores bearing two or four dansyl fluorophores	Pb(II)	19.3 nM	39
Salicylaldehyde phenyl-hydrazone fluorescent sensor	Pb(II)	630 nM	40
Anthrylazamacrocycles	Cd(II)	5 nM	41
Poly(azomethine-urethane) fluorescent sensor	Cd(II)	886 μM	42
Carbon dot nanohybrids (CD nanohybrids prepared from bamboo leaves)	Pb(II)	0.14 nM	45
Bi/g-C$_3$N$_4$	Pb(II), Cd(II)	17.5μg l^{-1} (156.2 nM) 8.1 μg l^{-1} (39.1nM)	46
PPy-AHNSA	Cr(VI), Pb(II), Cd(II)	1.4 nM 2.6 nM 2.7 nM	This work

4. CONCLUSIONS

In this work we investigated a new, electrosynthesized AHNSA-PPy fluorescent sensor, able to detect very low concentrations of Cr(VI), Pb(II) and Cu(II) ions in aqueous solutions. Our UV-VIS absorption and fluorescence spectral study of AHNSA-PPy demonstrated the existence of significant intermolecular interactions between the PPy chains and AHNSA naphthalenic groups, which were simply inserted between the PPy chains. When immersed in Cr(VI), Pb(II) or Cu(II) solutions, electrosynthesized AHNSA-PPy exhibited strong fluorescence quenching. Detailed analysis of the relationships based on the Stern-Volmer, Perrin, and polynomial equations showed that this AHNSA-PPy fluorescence quenching was essentially dynamic in the case of Cr(VI) ions but suggested the existence of a complex fluorescence quenching mechanism for Pb(II) and Cu(II) ions, implying a combination of dynamic and static fluorescence quenching. We evaluated the usefulness of AHNSA-PPy as a very sensitive quenching fluorimetric sensor for determining exceedingly low concentrations of Cr(VI), Pb(II) and Cd(II) ions in

the nM range. Therefore, AHNSA-PPy might be utilized for the detection of trace, toxic heavy metal ions in environmental samples.

REFERENCES

[1] G. F. Nordberg, Health hazards of environmental cadmium pollution, *Ambio,* **3**, 55–66 (1974).

[2] T. R. Sandrin, R. M. Maier, Impact of metals on the biodegradation of organic pollutants, *Environ. Health Perspect*, **111**, 1093–1101 (2003).

[3] J. O. Nriagu, J. M. Pacyna, Quantitative assessment of worldwide contamination of air, water and soils by trace metals, Nature, **333**, 134–139 (1988).

[4] D. E. Kimbrough, Y. Cohen, A. M. Winer, L. Creelman, C. Mabuni, A critical assessment of chromium in the environment, *Crit. Rev. Environ. Sci. Technol.*, **29**, 1–46 (1999).

[5] C. W. Randall, J. L. Barnard, H. D. Stensel (1992): *Design and retrofit of wastewater treatment plants for biological nutrient removal*. Technomic Publishing, USA.

[6] E. Watanabe, H. Endo, K. Toyama (1988) Determination of phosphate ions with an enzyme sensor system. Biosensors 3: 297–306.

[7]   H. Kawasaki, K. Sato, J. Ogawa, Y. Hasegawa, H. Yuki Determination of inorganic phosphate by flow injection method with immobilized enzymes and chemilumines-cence detection, *Anal. Biochem.,* **182**, 366–370 (1989).

[8]   S. J. Toal, K. A. Jones, D. Magde, W. C. Trogler, Lumi-nescent silole nanoparticles as chemoselective sensors for Cr(VI), *J. Amer. Chem. Soc.*, **127**, 11661–11665 (2005).

[9]   A. Ravindran, M. Elavarasi, T. C. Prathna, A. M. Rai-chur, N. Chandrasekaran, A. Mukherjee, Selective color-imetric detection of nanomolar Cr(VI) in aqueous solu-tions using unmodified silver nanoparticles, *Sensors Ac-tuators,* **B 166**, 365–371 (2012).

[10] S. Vallejos, A. Muñoz, F. C. García, F. Serna, S. Ibeas, J. M. García, Methacrylate copolymers with pendant pi-perazinedione-sensing motifs as fluorescent chemosen-sory materials for the detection of Cr(VI) in aqueous media, *J. Hazard Mater,* **227**, 480–483 (2012).

[11] J. M. Zachara, C. C. Ainsworth, G. E. Brown et al., Chromium speciation and mobility in a high level nucle-ar waste vadose zone plume, *Geochim. Cosmochim. Ac-ta*, **68**, 13–30 (2004).

[12] P. Sylvester, L. A. Rutherford, A. Gonzalez-Martin, J. Kim, Ferrate treatment for removing chromium from high-level radioactive tank waste, *Environ. Sci. Technol.* **35,** 216–221(2001).

[13] J.-P. Goullé, Métaux In: P. Kintz (ed), Toxicologie et Pharmacologie Médicolégales, Elsevier, Paris, pp. 189–232 (1998)

[14] L. Patrick, Lead toxicity Part II: the role of free radical damage and the use of antioxidants in the pathology and treatment of lead toxicity, *Altern. Med. Rev*., **11**, 114–127 (2006).

[15] R. G. Arnold, D. O. Carpenter, D. Kirk et al., Meeting report: threats to human health and environmental sus-tainability in the pacific basin, *Environ Health Perspect,* **115**, 1770–1775 (2007).

[16] L. Fewtrell, R. Kaufmann, A. Prüss (2003) Lead: as-sessing the environmental burden of diseases at national and local levels. Geneva. http://www.who.int/iris/handle /10665/42715.

[17] J.-P. Goullé, E. Saussereau, L. Mahieu, D. Bouige, M. Guerbet, C. Lacroix, Une nouvelle approche biologique : le profil métallique, *Ann. Biol. Clin*., **68**, 429–440 (2010).

[18] D. Bayersmann, S. Hechtenberg, Cadmium, gene regula-tion, and cellular signalling in mammalian cells, *Toxicol. Appl. Pharmacol*., **144**, 247–261 (1997).

[19] M. Satoh, T. Kaji, C. Tohyama, Low dose exposure to cadmium and its health effects. Part 3. Toxicity in labor-atory animals and cultured cells, *Nippon Eiseigaka Zas-shi*, 57, 615–623 (2003).

[20] B. E. Bengtsson, C. H. Carlin, Å. Larsson, O. Svanberg, Vertebral damage in minnows, Phoxinus phoxinus L. exposed to cadmium, Ambio, 4,166–168 (1975).

[21] Y. Mao, M. Hong, A. Liu, D. Xu, Highly selective and sensitive detection of Hg(II) from $HgCl_2$ by a simple rhodamine-based fluorescent sensor, *J. Fluoresc.*, 25, 755–761 (2015).

[22] S. Erdemir, O. Kocyigit, S. Malkondu, Fluorogenic recognition of Zn(II), Al(III) and F−ions by a new multi-

[23] Z. Zhang, C. Sha, A. Liu, Z. Zhang, D. Xu, Highly se-lective detection of Cr(VI) in water matrix by a simple 1,8-naphthalimide-based turn-on fluorescent sensor, *J. Fluoresc.*, 25, 335–340 (2015).

[24] J. Kim, Assemblies of conjugated polymers. intermolec-ular and intramolecular effects on the photophysical properties of conjugated polymers, *Pure Appl. Chem.*, **74**, 2031–2044 (2002).

[25] I. G. Scheblykin, A. Yartsev, T. Pullerits, V. Gulbinas, V. Sundstrm, Excited state and charge photogeneration dynamics in conjugated polymers, *J. Phys. Chem.*, B 111, 6303–6321 (2007).

[26] E. L. Cabarcos, S. A. Carter, Characterization of the photoluminescence quenching of mixed water-soluble conjugated polymers for potential use as biosensor mate-rials, *Macromolecules*, 38, 4409–4415(2005).

[27] L. Cisse, A. Djande, M. Capo-Chichi, F. Delattre, A. Saba, J.-C. Brochon, S. Sanouski, A. Tine, J.-J. Aaron, Fluorescence quenching of two coumarin-3-carboxylic acids by trivalent lanthanide ions, *J. Fluoresc.,* 27, 619–628 (2017).

[28] U. Lange, N. V. Roznyatovskaya, V. M. Mirsk, Con-ducting polymers in chemical sensors and arrays, *Anal. Chim. Acta.*, 614, 1–26 (2008).

[29] S.-N. Ding, S. Cosnier, M. Holzinger, X. Wang, Elec-trochemical fabrication of novel fluorescent polymeric film: Poly(pyrrole–pyrene), *Electrochem. Commun.*, **10**, 1423–1426 (2008).

[30] W. Ding, G. Zhang, H. Zhang, J. Xu, Y. Wen, J. Zhang, One step electrosynthesis of conjugated polymers thin film for Fe(III)detection and its potential application, *Sensors Actuators B –Chem.,* 237, 59–66 (2016).

[31] J. Maiti, B. Pokhrel, R. Boruah, S. K. Dolui, Polythio-phene based fluorescence sensors for acids and metal ions, *Sensors Actuators B-Chem.*, 141, 447–451 (2009).

[32] A. L. Holt, J. P. Bearinger, C. L. Evans, S. A. Carter, Chemically robust conjugated polymer platform for thin-film sensors, *Sensors Actuators B-Chem.*, 143, 600–605 (2010).

[33] C. Xing, Z. Shi, M. Yu, S. Wang, Cationic conjugated polyelectrolyte-based fluorometric detection of copper (II) ions in aqueous solution, *Polymer*, 49, 2698–2703 (2008).

[34] M. Lo, A. K. D Diaw, D. Gningue - Sall, M. A. Oturan, M. M. Chehimi, J.-J. Aaron, A novel fluorescent sensor based on electrosynthesized benzene sulfonic acid-doped polypyrrole for determination of Pb(II) and Cu(II), *Luminescence*, 34, 489–499 (2019). DOI: 10.1002 / bio.3626

[35] M. L. Sall, A. K. D Diaw, D. Gningue-Sall, A. Chevil-lot-Biraud, N. Oturan, M. A. Oturan, J.-J. Aaron, Re-moval of Cr(VI) from aqueous solution using electro-synthesized 4-amino-3- hydroxynaphthalene-1-sulfonic acid doped polypyrrole as adsorbent, *Environ. Sci. Pol-lut. Res.* 24, 21111–21127 (2017).

[36] M. L. Sall, A. K. D Diaw, D. Gningue-Sall et al., Re-moval of lead and cadmium from aqueous solutions by

using 4-amino-3-hydroxynaphthalene sulfonic acid-doped polypyrrole films, *Environ. Sci. Pollut. Res*., 25, 8581–8591 (2018).

[37] A. Adenier, J.-J. Aaron, A spectroscopic study of the fluorescence quenching interactions between biomedically important salts and the fluorescent probe merocyanine 540, *Spectrochim Acta* Part A, 58, 543–551 (2002).

[38] J. Afshani, A. Badiei, M. Karimi et al., A single fluorescent sensor for Hg(II) and discriminately detection of Cr(III) and Cr(VI), *J. Fluoresc.*, 26, 263–270 (2016).

[39] R. Métivier, I. Leray, B. Valeur, Lead and mercury sensing by calixarene-based fluoroionophores bearing two or four dansyl fluorophores, *Chem. Eur. J.*, 10, 4480–4490 (2004).

[40] D. K. Das, P. Goswami, S. Sarma, Salicylaldehyde phenylhydrazone: A new highly selective fluorescent lead (II) probe, *J. Fluoresc.* 23, 503–508 (2013).

[41] S. Charles, F. Dubois, S. Yunus, E. Vander Donckt, Determination by fluorescence spectroscopy of cadmium at the subnanomolar level: application to sea water. *J. Fluoresc.*, 10, 99–105 (2000).

[42] İ. Kaya, M. Kamaci, Highly selective and stable florescent sensor for Cd(II) based on poly(azomethine-urethane), *J. Fluoresc.*, 23, 115–121 (2013).

[43] Code of Federal Regulation. *Protection of Environment* (2011): Section 141, 80, Title [40], 425.

[44] *Edition of the Drinking Water Standards and Health Advisories, EPA 822-F-18-001,* Office of Water U.S. Environmental Protection Agency, Washington, DC, USA (2018).

[45] Z. Liu, W. Jin, F. Wang, T. Li, J. Nie, W. Xiao, Q. Zhang, Y. Zhang, Ratiometric fluorescent sensing of Pb^{2+} and Hg^{2+} with two types of carbon dot nanohybrids synthesized from the same biomass, *Sensors & Actuators: B. Chemical* **296**,126698 (2019). DOI: https://doi.org/10.1016/j.snb.2019.126698

[46] H. Zheng, L. Ntuli, M. Mbanjwa, N. Palaniyandy, S. Smith, M. Modibedi, K. Land, M. Mathe, The Effect of g-C3N4 Materials on Pb(II) and Cd(II) Detection Using Disposable Screen-Printed Sensors, (2018). DOI: https://doi.org/10.1007/s12678-018-0504-0